XLI CILAMCE
XLI Ibero-Latin American Congress on Computational Methods in Engineering
16-19 November, 2020 FOZ DO IGUAÇU PARANÁ – BRAZIL

PARAMETRIC STUDY ON FRACTURE ANGLE SEARCH ALGORITHM FOR PUCK'S 3D MATRIX FAILURE CRITERION

Kayque Andson S. Ximenes
Marcelo S. Medeiros Jr.
Evandro Parente Jr.
kayque.ximenes@gmail.com
marcelomedeiros@ufc.br
evandro@ufc.br
Laboratório Mecânica Computacional e Visualização , Universidade Federal do Ceará
Campus do Pici - Bloco 728, 60440-900, Fortaleza, CE - Brasil

Abstract. The Puck's failure criteria is one of the most successful models for assessing the onset of damage in unidirectional (UD) laminate composites. However the original algorithm proposed for matrix fracture plane angle search is based on brute-force approach where all the angles between -90^{o} to 90^{o}, in increments of 1^{o} ought to be evaluated. This work presents an enhanced method to expedite the detection of inter-fiber fracture (IFF) angle in UD laminate composites. A series of numerical optimisations and enhancements were made to reduce the computational cost of the fracture angle search.

Keywords: Unidirectional Laminate Composites, Puck's failure criteria, Inter-Fiber Failure, Fracture Angle Search, Optimisations.

1 Puck's Inter-Fiber matrix failure Criterion

The Puck inter-fiber fracture (IFF) criterion is based on the Mohr–Coulomb theory on isotropic materials which has been transferred to transverse isotropic brittle materials by Hashin [1]. It was postulated, that if the fracture plane can be identified, fracture will only be caused by normal and shear stresses σ_n, σ_{n1}, σ_{nt} acting on the fracture plane.

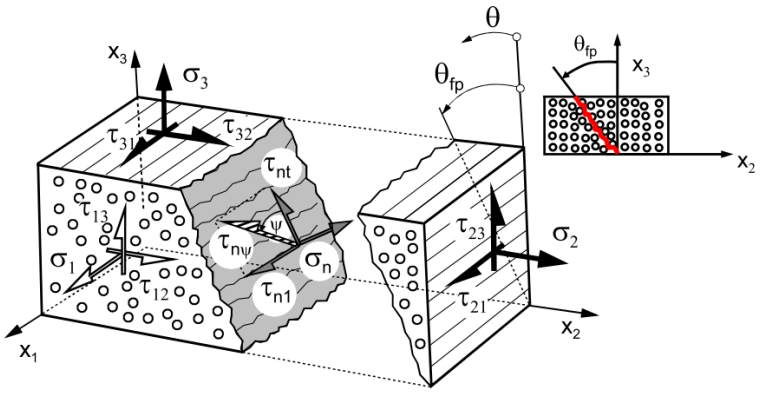

Figure 1. Stresses in the Fracture Plane. [2]

To calculate the stress state in an arbitrary fibre parallel "action plane", the stress state has to be transformed from the material coordinate system in the X_1, X_n, X_t system of the action plane, using the following equation:

$$\begin{Bmatrix} \sigma_1 \\ \sigma_n \\ \sigma_t \\ \tau_{nt} \\ \tau_{t1} \\ \tau_{n1} \end{Bmatrix} = \begin{bmatrix} 1 & 0 & 0 & 0 & 0 & 0 \\ 0 & c^2 & s^2 & 2sc & 0 & 0 \\ 0 & s^2 & c^2 & -2sc & 0 & 0 \\ 0 & -sc & sc & c^2 - s^2 & 0 & 0 \\ 0 & 0 & 0 & 0 & c & -s \\ 0 & 0 & 0 & 0 & s & c \end{bmatrix} \begin{Bmatrix} \sigma_{11} \\ \sigma_{22} \\ \sigma_{33} \\ \tau_{23} \\ \tau_{13} \\ \tau_{12} \end{Bmatrix} \tag{1}$$

Three-dimensional failure criteria of unidirectional fiber composites are established in terms of quadratic stress polynomials which are expressed in terms of the transversely isotropic invariants of the applied average stress state. [3–7]

From Eq.1 where $c = \cos(\theta)$ e $s = \text{sen}(\theta)$, can be obtained:

$$\begin{aligned} \sigma_n(\theta) &= \sigma_{22} \cdot cos^2(\theta) + \sigma_{33} \cdot sen^2(\theta) + \tau_{23} \cdot 2sen(\theta) cos(\theta) \\ \tau_{n1}(\theta) &= \tau_{12} \cdot cos(\theta) + \tau_{13} \cdot sen(\theta) \\ \tau_{nt}(\theta) &= -\sigma_{22} \cdot sen(\theta) cos(\theta) + \sigma_{33} \cdot sen(\theta) cos(\theta) + \tau_{23} \cdot \left[cos^2(\theta) - sen^2(\theta)\right] \\ \tau_{n\psi} &= \sqrt{(\tau_{nt})^2 + (\tau_{nl})^2} \end{aligned} \tag{2}$$

Puck's criterion for IFF is divided into two equations. The first is created when σ_n is positive:

$$f_{E_{FF}}(\theta) = \sqrt{\left[\left(\frac{1}{R_{\perp}^{At}} - \frac{p_{\perp\psi}^{t}}{R_{\perp\psi}^{A}}\right)\sigma_n(\theta)\right]^2 + \left(\frac{\tau_{nt}(\theta)}{R_{\perp\perp}^{A}}\right)^2 + \left(\frac{\tau_{n1}(\theta)}{R_{\perp\parallel}^{A}}\right)^2} + \frac{p_{\perp\psi}^{t}}{R_{\perp\psi}^{A}}\sigma_n(\theta) \tag{3}$$

The second is used for σ_n negative:

$$f_{E_{IFF}}(\theta) = \sqrt{\left(\frac{p_{\perp\psi}^{c}}{R_{\perp\psi}^{A}}\sigma_n(\theta)\right)^2 + \left(\frac{\tau_{nt}(\theta)}{R_{\perp\perp}^{A}}\right)^2 + \left(\frac{\tau_{n1}(\theta)}{R_{\perp\parallel}^{A}}\right)^2} + \frac{p_{\perp\psi}^{c}}{R_{\perp\psi}^{A}}\sigma_n(\theta) \tag{4}$$

where:

$$
\begin{aligned}
&PTR = \frac{p^t_{\perp\psi}}{R^A_{\perp\psi}} = \frac{p^t_{\perp\perp}}{R^A_{\perp\perp}}\cos^2\psi + \frac{p^t_{\perp\parallel}}{R^A_{\perp\parallel}}\sin^2\psi \;\; ; \;\; PCR = \frac{p^c_{\perp\psi}}{R^A_{\perp\psi}} = \frac{p^c_{\perp\perp}}{R^A_{\perp\perp}}\cos^2\psi + \frac{p^c_{\perp\parallel}}{R^A_{\perp\parallel}}\sin^2\psi \\
&\cos^2\psi = \frac{\tau^2_{nt}}{\tau^2_{nl}+\tau^2_{nt}} \;\; ; \;\; \sin^2\psi = \frac{\tau^2_{nl}}{\tau^2_{nl}+\tau^2_{nt}} \\
&R^A_{\perp\psi} = \left[\left(\frac{\cos\psi}{R^A_{\perp\perp}}\right)^2 + \left(\frac{\sin\psi}{R^A_{\perp\parallel}}\right)^2\right] \Rightarrow R^A_{\perp\psi} = \left[\frac{\tau^2_{nt}\left(R^A_{\perp\parallel}\right)^2 + \tau^2_{nl}\left(R^A_{\perp\perp}\right)^2}{\left(R^A_{\perp\perp}\right)^2\left(\tau^2_{nl}+\tau^2_{nt}\right)\left(R^A_{\perp\parallel}\right)^2}\right] \\
&\text{RVVA} = R^A_{\perp\perp} = \frac{R^c_{\perp}}{2(1+p^c_{\perp\perp})} \;\; ; \;\; R^{At}_{\perp} = R^A_{\perp} = R^{(+)}_{\perp} = R^t_{\perp} = Y_T \;\; ; \;\; R^{(-)}_{\perp} = R^c_{\perp} = Y_C \\
&R^A_{\perp\parallel} = R_{\perp\parallel} = S_{21} \;\; ou \;\; \frac{p^c_{\perp\perp}}{R^A_{\perp\perp}} = \frac{p^c_{\perp\parallel}}{R_{\perp\parallel}} \Rightarrow R_{\perp\parallel} = \frac{p^c_{\perp\parallel}\cdot R^A_{\perp\perp}}{p^c_{\perp\perp}}
\end{aligned}
\tag{5}
$$

$R^{At}_{\perp}$ and $R^A_{\perp\parallel}$ are the tensile strengths perpendicular to the fibers and the shear strength in the plane respectively, $R^A_{\perp\perp}$ is the fracture strength due to the transversal/transverse shearing. θ is the angle of the analyzed plane and $f_{E_{IFF}}$ is the exposure to fracture stresses between the fibers of the blade, which when equal to 1 indicates the fracture of the blade. $p^{t,c}_{\perp\parallel}$ and $p^{t,c}_{\perp\perp}$ are slope parameters, which are obtained through the curves of σ_{22}, τ_{21}. However, they are difficult to obtain without performing a series of experiments, so Puck recommends certain values of these slope parameters, in the case of carbon fiber: $p^c_{\perp\parallel} = 0.3$, $p^t_{\perp\parallel} = 0.35$ e $p^{t,c}_{\perp\perp} = 0.3$ [2].

It is important to explain that PTR, PCR and RVVA are nomenclatures used in this work to simplify the expressions and the declaration of variables in the UMAT code. For a better understanding of the code, this nomenclaura was introduced in Equation (5) and replaced in Equations (3) and (4). In comparison with the index nomenclature, which is normally used, adopted $\parallel$ corresponding to and $\perp$ ao 2, in other words, $p^c_{\perp\parallel} = P21C$, $p^t_{\perp\parallel} = P21T$, $p^t_{\perp\perp} = P22T$ and $p^c_{\perp\perp} = P22C$. YT, YC and S_{21} are nomenclatures already used in other works similar to this one, such as Wiegand2008.

Using the relationships exposed in the Equation 5, the Equation 3 e 4 can be simplified to:

σ_n positive:

$$
f_{E_{IFF}}(\theta) = \sqrt{\left[\left(\frac{1}{Y_T} - PTR\right)\sigma_n(\theta)\right]^2 + \left(\frac{\tau_{nt}(\theta)}{RVVA}\right)^2 + \left(\frac{\tau_{nl}(\theta)}{S_{21}}\right)^2} + PTR\cdot\sigma_n(\theta) \tag{6}
$$

σ_n negative:

$$
f_{E_{IFF}}(\theta) = \sqrt{\left[PCR\cdot\sigma_n(\theta)\right]^2 + \left(\frac{\tau_{nt}(\theta)}{RVVA}\right)^2 + \left(\frac{\tau_{nl}(\theta)}{S_{21}}\right)^2} + PCR\cdot\sigma_n(\theta) \tag{7}
$$

When σ_n is a tensile stress, it promotes the IFF by helping with the shear stress, but if σ_n is compression, it delays the occurrence of the IFF, as it increases the fracture resistance against fracture because of this, separate equations are necessary for both cases.

θ_{fp} is the angle of the fracture plane, that is, the plane where there is the greatest risk of fracture occurring. This angle, in the original Puck model, is determined by calculating $f_{E_{IFF}}(\theta)$ for all values between $\theta = 90^{\circ}$ to $\theta = -90^{\circ}$, with steps of 1°. Thus, the plane with the greatest exposure to stresses is the plane in which the fracture is expected, $[f_{E_{IFF}}(\theta)]_{\max} = f_{E_{IFF}}(\theta_{fp})$.

However, this method of searching the fracture angle causes a great computational cost, since at each step it is necessary to perform around 180 interactions. So, in this work, this search process was modified, implementing simplified methods of numerical optimization.

2 Optimisation of Fracture Angle Search

In order to reduce the number of interactions in the search for the fracture angle and, consequently, the computational cost of an analysis, some improvements were made to the Puck criterion.

The first improvement applied was the delimitation of the angle search space. Analyzing Equations 6 and 7, it can be seen that the elements linked to θ are σ_n, τ_{nt} and τ_{nl}. Then we tried to find the angles corresponding to the maximum stress σ_n, τ_{nt} and τ_{nl}. For this, each of the expressions in Equation 2 was simplified into a single sinusoidal function of θ, using basic trigonometric relations and overlapping concepts of sine waves of the same frequency, which allow combining two sine waves into a single cosine, Equation 8.

$$\begin{aligned} Acos\left(\theta+\alpha\right)+Bcos\left(\theta+\beta\right) =& \sqrt{\left[Acos\left(\alpha\right)+Bcos\left(\beta\right)\right]+\left[Asen\left(\alpha\right)+Bsen\left(\beta\right)\right]} \\ & \times\ cos\left(\theta+tan^{-1}\left[\frac{Asen\left(\alpha\right)+Bsen\left(\beta\right)}{Acos\left(\alpha\right)+Bcos\left(\beta\right)}\right]\right) \end{aligned} \tag{8}$$

The resulting expressions, given below, separates the effect of stresses from the effect of the angle of rotation to some extent, allowing for a clearer interpretation of the three stresses of the fracture plane that define the probability of failure in Puck's IFF criterion.

$$\begin{aligned} \sigma_n &= \left(\tfrac{\sigma_{22}+\sigma_{33}}{2}\right)+\sqrt{\left(\tfrac{\sigma_{22}-\sigma_{33}}{2}\right)^2+\left(\tau_{23}\right)^2}\ \cdot\ cos\left(2\theta+tan^{-1}\left[\tfrac{-2\tau_{23}}{\sigma_{22}-\sigma_{33}}\right]\right) \\ \tau_{nl} &= \sqrt{\left(\tau_{12}\right)^2+\left(\tau_{13}\right)^2}\ \cdot\ cos\left(\theta+tan^{-1}\left[\tfrac{\tau_{13}}{\tau_{13}}\right]\right) \\ \tau_{nt} &= \sqrt{\left(\tfrac{\sigma_{22}-\sigma_{33}}{2}\right)^2+\left(\tau_{23}\right)^2}\ \cdot\ cos\left(2\theta+tan^{-1}\left[\tfrac{|\sigma_{22}-\sigma_{33}|}{2\tau_{23}}\right]\right) \end{aligned} \tag{9}$$

For type $Acos(n\theta+\alpha)+C$ sinusoidal waves, as in Equation 9, the maximum point is defined by its phase shift -α/n, and its value at this point is the sum of the amplitude with vertical displacement, A + C. Applying this solution to the expressions Equation 9 gives the expressions of the maximum stress of the fracture plane and the respective angles in which each one occurs, Equation 10.

$$\begin{aligned} \theta_1 = \tfrac{1}{2}tan^{-1}\left(\tfrac{2\tau_{23}}{\sigma_{22}-\sigma_{33}}\right) &\Rightarrow \sigma_n^{MAX} = \left(\tfrac{\sigma_{22}+\sigma_{33}}{2}\right)+\sqrt{\left(\tfrac{\sigma_{22}-\sigma_{33}}{2}\right)^2+\left(\tau_{23}\right)^2} \\ \theta_{2,3} = \theta_1\ \overline{+}\ \tfrac{\pi}{4} &\Rightarrow \tau_{nt}^{MAX} = \sqrt{\left(\tfrac{\sigma_{22}-\sigma_{33}}{2}\right)^2+\left(\tau_{23}\right)^2} \\ \theta_4 = -tan^{-1}\left(\tfrac{\tau_{13}}{\tau_{12}}\right) &\Rightarrow \tau_{nl}^{MAX} = \sqrt{\left(\tau_{12}\right)^2+\left(\tau_{13}\right)^2} \end{aligned} \tag{10}$$

The angles calculated by the expressions of Equation 10 correspond to the maximum only for their respective tension. The angle of the fracture plane is the angle referring to the global maximum of the Equation $f_{E_{IFF}}\left(\theta\right)$, which is an interaction of the three stresses. However, these angles will serve to delimit the angle search space, as explained previously. This delimitation is done by choosing, from the four values of θ_1 to θ_4, the two angles that have the two largest values of $f_{E_{IFF}}\left(\theta\right)$, where the first largest will be the upper limit and the second largest will be the lower limit.

After this delimitation, the second improvement is made, which consists of applying a simplified optimization method, replacing the process of calculating the value of $f_{E_{IFF}}$ for each angle, varying from 1 in 1st degree.

The method applied was the Brent method, which consists of the alternating combination of the Golden-Section method and the parabolic interpolation method [8]. This combination is interesting because, after some interactions, when the upper and lower limits are very close, the Golden-Section method starts to perform many interactions to converge to an exact point. Then, when it reaches a certain tolerance, it changes to the Parabolic Interpolation method which converges much faster.

The Golden-Section search method is a technique in which the extreme is found by successively narrowing the search interval. Each interaction or "narrowing" is done by analyzing four points $theta_l$

(lower limit), θ_u (upper limit), θ_{l+d} and θ_{ud}, where:

$$\begin{gathered}\phi = \frac{1+\sqrt{5}}{2} \quad e \quad d = (\phi - 1)(x_u - x_l) \\ \theta_{l+d} = \theta_l + d \;\; e \;\; \theta_{u-d} = \theta_u - d\end{gathered} \tag{11}$$

Then $f_{E_{IFF}}(\theta_{l+d})$ and $f_{E_{IFF}}(\theta_{u-d})$ values are calculated and analyzed. In a case of maximization, as it is in this work, if $f_{E_{IFF}}(\theta_{l+d})$ ¿ $f_{E_{IFF}}(\theta_{u-d})$, updates θ_l = θ_{u-d} and θ_{opt} = θ_{l+d} keeping θ_u, and if $f_{E_{IFF}}(\theta_{u-d})$ ¿ $f_{E_{IFF}}(\theta_{l+d})$, updates θ_u = θ_{l+d} and θ_{opt} = θ_{u-d} keeping θ_l. θ_{opt} is the optimal value of each interaction, that is, the maximum point of each interaction and it is used to calculate the error given by the Equation 12.

$$erro_{GS} = (2 - \phi)\left|\frac{\theta_u - \theta_l}{\theta_{opt}}\right| \tag{12}$$

Upon reaching the proposed error tolerance, the Parabolic Interpolation method is used, using the points θ_l, θ_u and θ_{opt} from the last Golden-Section interaction and their respective values in the function. With these data it is possible to obtain a parable using the following equation:

$$\begin{aligned}p(\theta) =& f_{E_{IFF}}(\theta_l)\frac{(\theta - \theta_u)(\theta - \theta_{opt})}{(\theta_l - \theta_u)(\theta_l - \theta_{opt})} + f_{E_{IFF}}(\theta_u)\frac{(\theta - \theta_l)(\theta - \theta_{opt})}{(\theta_u - \theta_l)(\theta_u - \theta_{opt})} \\ &+ f_{E_{IFF}}(\theta_{opt})\frac{(\theta - \theta_l)(\theta - \theta_u)}{(\theta_{opt} - \theta_l)(\theta_{opt} - \theta_u)}\end{aligned} \tag{13}$$

Since this process is subsequent to the narrowing of the Golden-Section method, the maximum of $p(\theta)$ is normally sufficiently close to the maximum of $f_{E_{IFF}}(\theta)$, then the following approach can be adopted:

$$\theta_{max} = \theta_u - \frac{1}{2}\frac{(\theta_u - \theta_l)^2\left(f_{E_{IFF}}(\theta_u) - f_{E_{IFF}}(\theta_{opt})\right) - (\theta_u - \theta_{opt})^2\left(f_{E_{IFF}}(\theta_u) - f_{E_{IFF}}(\theta_l)\right)}{(\theta_u - \theta_l)\left(f_{E_{IFF}}(\theta_u) - f_{E_{IFF}}(\theta_{opt})\right) - (\theta_u - \theta_{opt})\left(f_{E_{IFF}}(\theta_u) - f_{E_{IFF}}(\theta_l)\right)} \tag{14}$$

the maximum point of the parabola is calculated and updates the value of θ_{opt} = θ_{max}. Se θ_{opt} ¿ θ_{max}, it is done θ_u = θ_{opt} and if θ_{opt} ¡ θ_{max}, it is done θ_l = θ_{opt}. Then the process is repeated until the tolerance is reached by the error, which is calculated as follows:

$$erro_{IP} = \left|\frac{\theta_{max} - \theta_{opt}}{\theta_{max}}\right| \tag{15}$$

The third improvement is to avoid unnecessary search for the fracture angle. Normally, analyzes are performed by applying load or displacement control, which consists of adding load or displacement to each step of the analysis. In the first steps, the stresses will be low and as Puck's criterion uses the stresses, there would be no damage. Then a criterion was defined to help distinguish when the stresses are large enough to justify a complete assessment of the failure criterion, reducing the number of times the angle search is performed. Using the maximums of the three stresses of the fracture plane, described in Equation **??**, one can adapt Equation 6 to describe an upper boundary case scenario.

$$f_{E_{Lim}} = \sqrt{\left[\left(\frac{1}{Y_T} - PTR\right)\sigma_n^{MAX}\right]^2 + \left(\frac{\tau_{nt}^{MAX}}{R_{\perp\perp}^A}\right)^2 + \left(\frac{\tau_{nl}{}^{MAX}}{S_{21}}\right)^2} + PTR \cdot \sigma_n \tag{16}$$

$f_{E_{Lim}}$ does not depend on θ so it can be calculated directly and immediately. By definition $f_E \leq f_{E_{Lim}}$, so if $f_{E_{Lim}} < 1$ then $f_E < 1$, which means that the possibility of failure in the given voltage state can be dismissed immediately without the need to search for the angle. In this way, the complete evaluation of the IFF criterion can be avoided by a large number of steps.

Finally, once the exposure, Fe, reaches 1, indicating the beginning of the failure, it is assumed that the fracture plane remains constant, that is, the fracture angle does not change and, therefore, the search for the angle is not more accomplished. The last improvement being the implementation of a conditional that when $f_E = 1$, the θ_{fr} is maintained and the algorithm does not enter the angle search process.

3 Results

The optimized search code was initially tested in an isolated way in order to verify the precision, regarding the maximum point value, and the efficiency, regarding the number of interactions necessary for the convergence. To test it, it were used curves described by the Equations (6) and (7), applying different stress states and their respective material parameters, in order to verify the effectiveness of the method. The stress state of each example is described in each figure and the parameters are YT = 59.1, YC = 231.2, P21C = P22T = P22C = 0.30, P21T = 0.33, RVVA = 88.923 e S_{21} = 98.4. In addition, iterations for convergence were counted in order to verify efficiency. The results are shown in the following figures and in the Table 1.

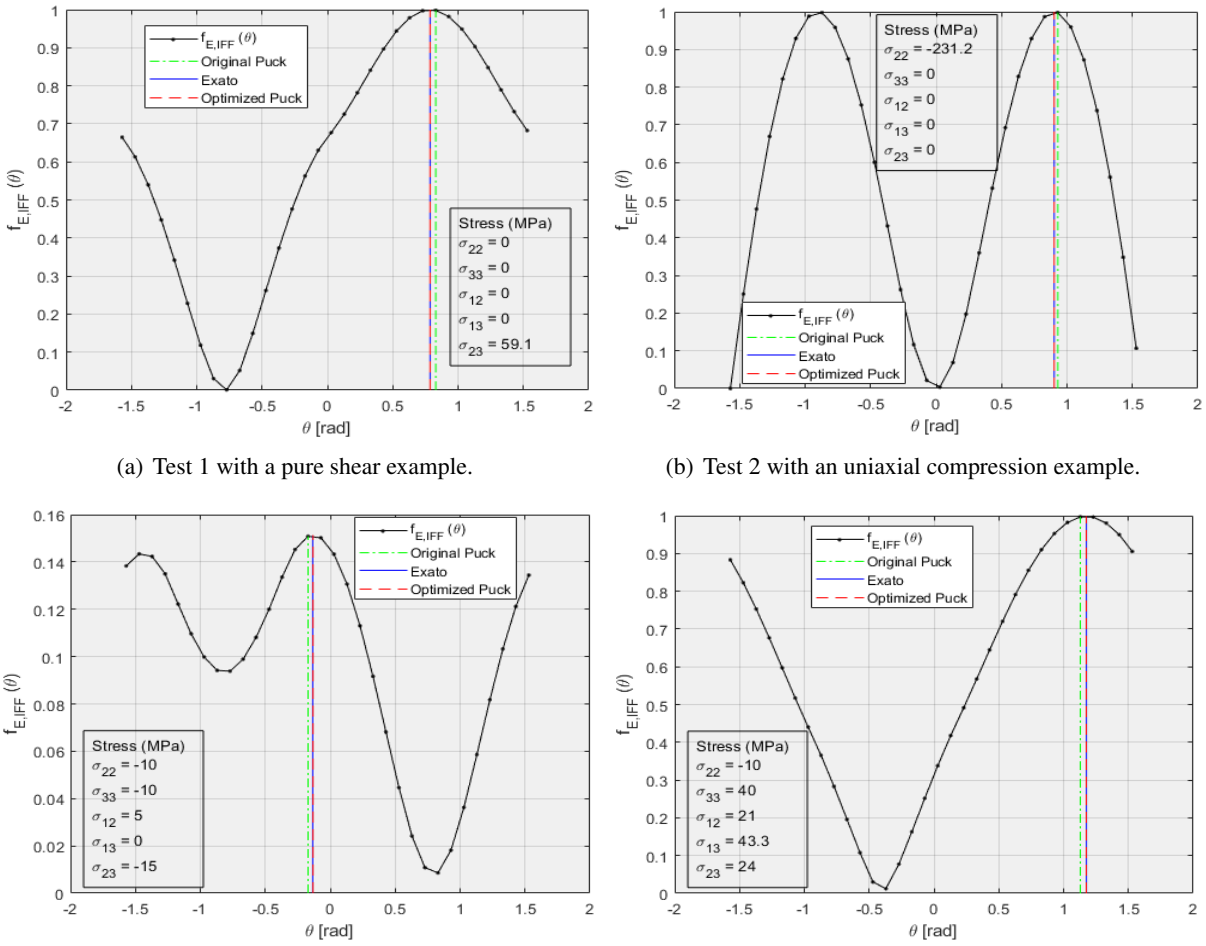

(a) Test 1 with a pure shear example.

(b) Test 2 with an uniaxial compression example.

(c) Test 3 with an arbritary stress state 3D example.

(d) Test 4 with an arbritary stress state 3D example.

Figure 2. Test curves of the algorithm and their respective stress states.

Table 1. Fracture angle search results

Test	Iterations	Exact		Puck Org.		Puck Opt.		Error	Error
		θ	$f_{E,IFF}(\theta)$	θ	$f_{E,IFF}(\theta)$	θ	$f_{E,IFF}(\theta)$	Org.[%]	Opt.[%]
1	12	0.7854	1.00000	0.8292	0.99830	0.7854	1.00000	0.1700	0.0000
2	14	0.9022	1.00000	0.9292	0.99820	0.9024	1.00000	0.1800	0.0000
3	19	-0.1343	0.15133	-0.1708	0.1509	-0.1326	0.1513	0.2872	0.0229
4	11	1.1768	0.99844	1.1292	0.99680	1.1755	0.99840	0.1642	0.0040

The applied method is simple and usually used for unimodal situations. However, the limited search space and some conditions described in the code have led all cases to converge to the global maximum.

As for efficiency, in all cases, more than 10 interactions were required, the desired limit. It is worth mentioning that this method is formed by the consecutive joining of two other methods, so a limit of 20 interactions can be considered, 10 of each sub-method. Thus, it can be said that all cases were within the limit. In addition, when compared to the number of interactions required by the conventional Puck method, 180 interactions, it showed excellent efficiency.

After being tested, the optimized search method was incorporated into the UMAT code for material degradation and validated using the long plate model with a centralized circular hole and subjected to uniformly distributed traction on the two side edges, the dimensions of which are described in the figure below .

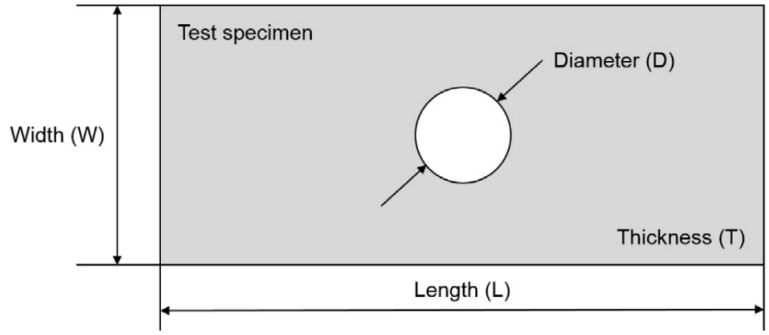

Dimensions and ply orientations of test specimen.

Laminate layup	D (mm)	W (mm)	T (mm)	L (mm)
$[0/(\pm 45)_3/(90)_3]_S$	6.35	25.4	2.616	203.2

Figure 3. Geometric properties of the modeled plate.

The modeled plate is a laminated composite consisting of epoxy resin type 1034-C and carbon fibers T300, whose properties are described in the following table. The lamination arrangement is $[0/(\overset{-}{+}45)_3/(90)_3]_S$, where each blade is 0.1308 mm.

Table 2. Material properties of T300 / 1304-C carbon fibers.

Property	E_{11} (MPa)	E_{22} (MPa)	G_{12} (MPa)	ν_{12}	ν_{23}	E_{f1} (MPa)	ν_{f12}
T300/1304-C	146.858	11.376	6185	0.3	0.28	230,000	0.2
Property	ϵ_{1T} (%)	ϵ_{1c} (%)	X_T (MPa)	X_C (MPa)	Y_T (MPa)	Y_C (MPa)	S_{12} (MPa)
T300/1304-C	1.807	0.652	1731	1379	67	268	58.7

This example was taken from the work of [2], which shows the ultimate stress obtained experimentally. [9] and [10] have also studied this same example and provided the force-displacement curves of their models. With the model developed in this work, the last load of 15.21 KN was obtained with the EWM method [11], with the 0º orientation blade being the last to break, figure 4. With the CSE method [2], the last load of 19.11 KN was obtained and the last blades to break were the 45º and 90º orientation.

Having the last load, the last stress was calculated by $\sigma_u = P_u \cdot (W \cdot T)$, obtaining for CSE σ_u = 287.6 and for EWM σ_u = 228.9. Comparing with the ultimate stress of 235.8 obtained experimentally, there is a lag of 22 % for the CSE and 2.9 % for the EWM. As for the behavior, it can be analyzed by means of figure 5, which contains the force x displacement curves of the models of this work and of the models of [9] and [10].

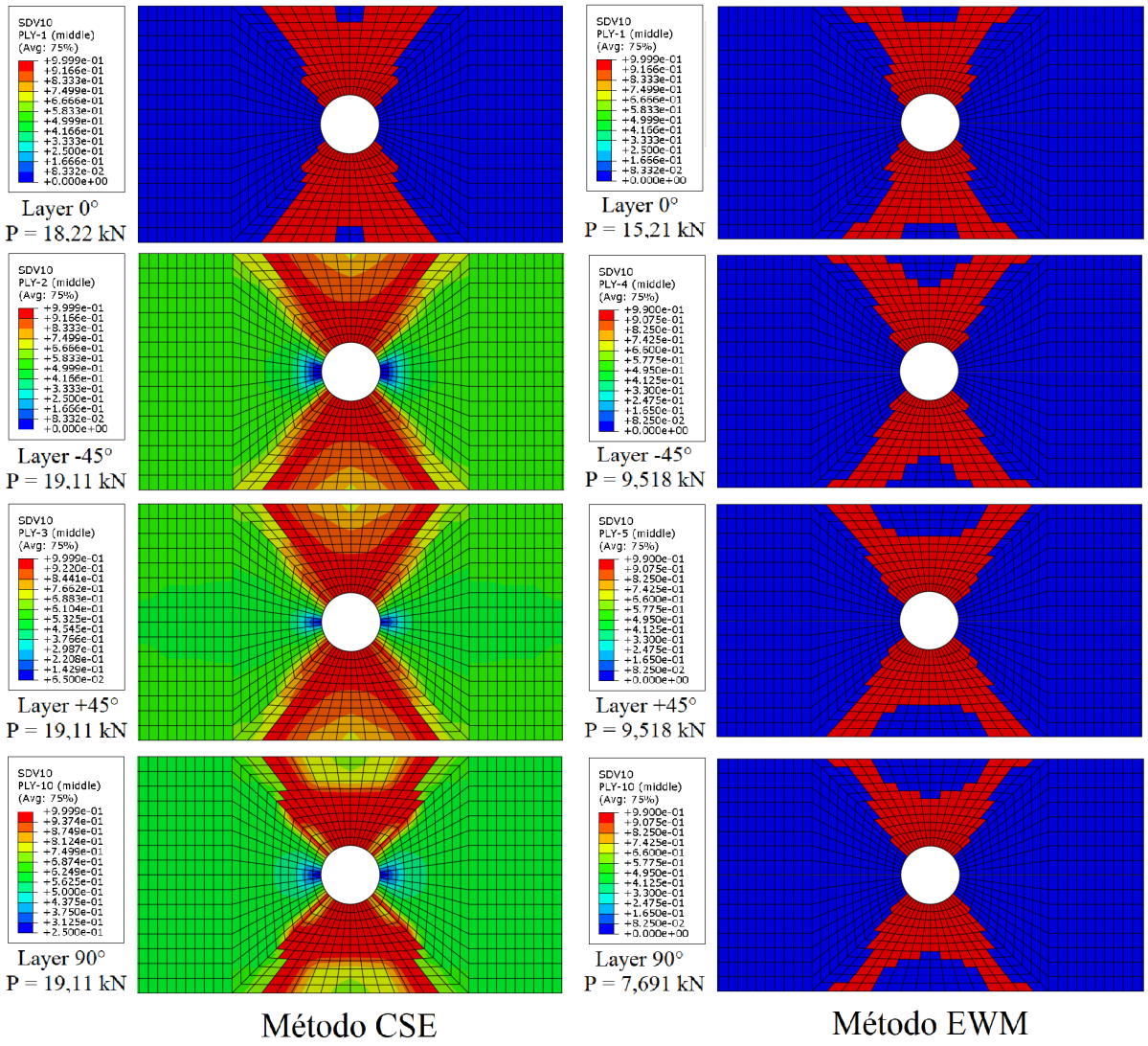

Figure 4. Damage Evolution.

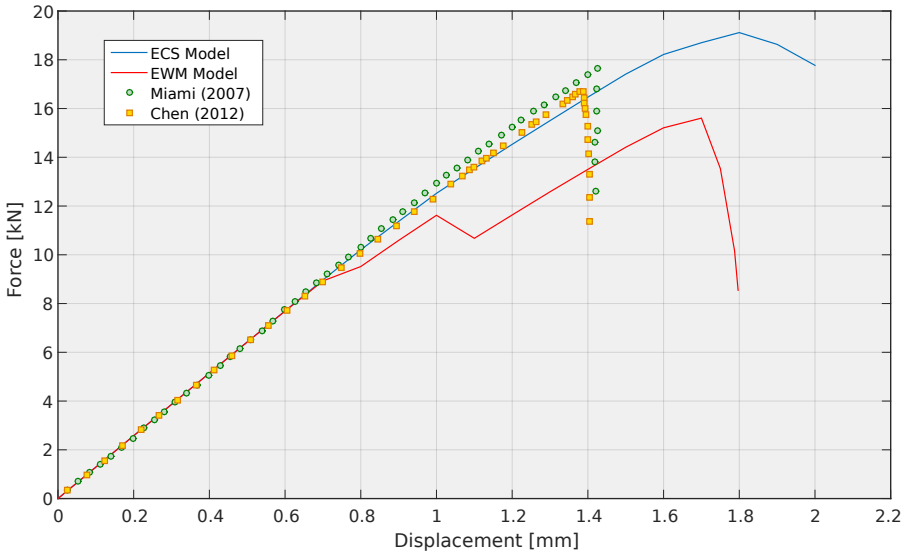

Figure 5. Force x Displacement Curves.

So, finally, the processing time was compared to check the efficiency of the code optimization. With the EWM model, the processing time without optimization was 1.745" and 930" with optimization. For the CSE model, the processing time without optimization was 1.602" and 582" with optimization. With the optimization there was a reduction of 815" (46,7%), in the EWM, and 1.020" (63,37%), in the CSE. Regarding the number of interactions in the search for the fracture angle, there was a reduction from 180 in the traditional search to 25 in the optimized search in this model.

Conclusions

In view of these results, the applied method can be considered admissible. The optimization applied to the search process provided good results, reducing, on average, by 50% the processing time. The adaptation of the use of the two angles with a higher stress factor to delimit the search space provided a greater direction for the global maximum. This allowed a unimodal optimization method to be effective in a multimodal situation. In one of the examples shown, the limiters directed the search to the global maximum, but did not include the maximum point in the search space. To resolve this situation, a scan similar to that applied to the original Puck method could be performed. In this case, however, the scan would be small, due to the proximity to the maximum point, and would not affect the efficiency of the optimization. As for the results of the analysis, it can be seen that this optimization did not interfere in the robustness of the models, offering an interesting solution with precision and lower computational cost.

Acknowledgements

The authors gratefully acknowledge the financial support provided by CNPq (Conselho Nacional de Desenvolvimento Científico e Tecnológico) and FUNCAP (Fundação Cearense de Apoio ao Desenvolvimento Científico e Tecnológico). They are also grateful to the scientific support of the LMCV (Laboratório de Mecânica Computacional e Vizualização) linked to UFC (Universidade Federeal do Ceará).

References

[1] Hashin, Z., 1980. Failure criteria for unidirectional fiber composites. *Journal of Applied Mechanics*, vol. 47, n. 2, pp. 329–334.

[2] Kodagali, K., 2017. *Progressive Failure Analysis of composite Materials using the Puck Failure Criteria*. Doctoral dissertation, University of South Carolina.

[3] Wiegand, J., Petrinic, N., & Elliott, B., 2008. An algorithm for determination of the fracture angle for the three-dimensional puck matrix failure criterion for UD composites. *Composites Science and Technology*, vol. 68, n. 12, pp. 2511–2517.

[4] Schirmaier, F., Weiland, J., Kärger, L., & Henning, F., 2014. A new efficient and reliable algorithm to determine the fracture angle for puck's 3d matrix failure criterion for UD composites. *Composites Science and Technology*, vol. 100, pp. 19–25.

[5] Deveci, H. A., Aydin, L., & Artem, H. S., 2016. Buckling optimization of composite laminates using a hybrid algorithm under puck failure criterion constraint. *Journal of Reinforced Plastics and Composites*, vol. 35, n. 16, pp. 1233–1247.

[6] Thomson, D. M., Cui, H., Erice, B., Hoffmann, J., Wiegand, J., & Petrinic, N., 2017. Experimental and numerical study of strain-rate effects on the IFF fracture angle using a new efficient implementation of puck's criterion. *Composite Structures*, vol. 181, pp. 325–335.

[7] Dutra, T. A., Ferreira, R. T. L., Resende, H. B., Blinzler, B. J., & Larsson, R., 2020. Expanding puck and schürmann inter fiber fracture criterion for fiber reinforced thermoplastic 3d-printed composite materials. *Materials*, vol. 13, n. 7, pp. 1653.

[8] Mohammadi, M. H., Silva, R. C. P., & Lowther, D. A., 2017. Finding optimal performance indices of synchronous AC motors. *IEEE Transactions on Magnetics*, vol. 53, n. 6, pp. 1–4.

[9] Chen, J. F., Morozov, E. V., & Shankar, K., 2012. A combined elastoplastic damage model for progressive failure analysis of composite materials and structures. *Composite Structures*, vol. 94, pp. 3478–3489.

[10] P.Miamí, Camanho, P. P., Mayugo, J. A., & Dávila, C. G., 2007. A continuum damage model for composite laminates: part ii – computacional implementation and validation. *Mechanics of Materials*, vol. 39, pp. 909–919.

[11] Lee, C.-S., Kim, J.-H., kee Kim, S., Ryu, D.-M., & Lee, J.-M., 2015. Initial and progressive failure analyses for composite laminates using puck failure criterion and damage-coupled finite element method. *Composite Structures*, vol. 121, pp. 406–419.